COMMUNICATIONS IN NUMERICAL METHODS IN ENGINEERING
Commun. Numer. Meth. Engng 2009; **25**:827–836
Published online 23 September 2008 in Wiley InterScience (www.interscience.wiley.com). DOI: 10.1002/cnm.1185

Non-locking tetrahedral finite element for surgical simulation

Grand Roman Joldes*,†, Adam Wittek and Karol Miller

Intelligent Systems for Medicine Laboratory, School of Mechanical Engineering, The University of Western Australia, 35 Stirling Highway, Crawley/Perth, WA 6009, Australia

SUMMARY

To obtain a very fast solution for finite element models used in surgical simulations, low-order elements, such as the linear tetrahedron or the linear under-integrated hexahedron, must be used. Automatic hexahedral mesh generation for complex geometries remains a challenging problem, and therefore tetrahedral or mixed meshes are often necessary. Unfortunately, the standard formulation of the linear tetrahedral element exhibits volumetric locking in case of almost incompressible materials. In this paper, we extend the average nodal pressure (ANP) tetrahedral element proposed by Bonet and Burton for a better handling of multiple material interfaces. The new formulation can handle multiple materials in a uniform way with better accuracy, while requiring only a small additional computation effort. We discuss some implementation issues and show how easy an existing Total Lagrangian Explicit Dynamics algorithm can be modified in order to support the new element formulation. The performance evaluation of the new element shows the clear improvement in reaction forces and displacements predictions compared with the ANP element in case of models consisting of multiple materials. Copyright © 2008 John Wiley & Sons, Ltd.

Received 4 May 2007; Accepted 18 August 2008

KEY WORDS: non-locking tetrahedron; surgical simulation; soft tissues; Total Lagrangian formulation

1. INTRODUCTION

Finite element models needed in surgical simulation must be both fast and accurate. In order to be fast, they must use low-order elements that are not computationally intensive, such as the linear tetrahedron or the linear under-integrated hexahedron. In order to be accurate, the generated mesh should approximate well the real geometry so that the boundary conditions can be imposed

*Correspondence to: Grand Roman Joldes, Intelligent Systems for Medicine Laboratory, School of Mechanical Engineering, The University of Western Australia, 35 Stirling Highway, Crawley/Perth, WA 6009, Australia.
†E-mail: grandj@mech.uwa.edu.au

Contract/grant sponsor: Australian Research Council, Discovery Project; contract/grant numbers: DP0343112, DP0664534, LX0560460
Contract/grant sponsor: NIH; contract/grant number: 1-RO3-CA126466-01A1
Contract/grant sponsor: UWA Research Grant

accurately. Many algorithms are now available for fast and accurate automatic mesh generation using tetrahedral elements, but not for automatic hexahedral mesh generation [1–3]. Therefore, in order to automate the simulation process, tetrahedral or mixed meshes are more convenient. Unfortunately, the standard formulation of the tetrahedral element exhibits volumetric locking, especially in case of soft tissues such as the brain, which are modeled as almost incompressible materials [4–10].

A number of improved linear tetrahedral elements were proposed by different authors [11–14]. The average nodal pressure (ANP) tetrahedral element proposed by Bonet and Burton in [11] is computationally inexpensive and provides much better results for nearly incompressible materials than the standard tetrahedral element. Nevertheless, one problem with the ANP element and its implementation in a finite element code is the handling of interfaces between different materials. In this paper, we extend the formulation of the ANP element so that all elements in a mesh are treated in a similar way, requiring no special handling of the interface elements.

When organs such as the brain are meshed using a mixed mesh, most of the tetrahedral elements are situated at the interface between the different parts of the brain (ventricle, tumor, white matter, gray matter), as these irregular sections are harder to mesh using only hexahedral elements. Therefore, the correct handling of the interface between different materials is very important.

We will show how this element formulation can be easily programmed in an existing finite element code [15] and present a deformation example that proves the increased performances of this element over the standard linear tetrahedron and the ANP elements.

This paper is organized as follows: the new element formulation is presented in Section 2; the integration in an existing finite element code is presented in Section 3; a computational example demonstrates the efficiency of the improved element in Section 4; and the conclusions are presented in Section 5.

2. IMPROVED ANP ELEMENT FORMULATION

2.1. Existing ANP formulation

We will start the development of the improved ANP (IANP) element by briefly presenting the standard ANP formulation developed in [11]. The volume attached to a node a is computed by adding the contributions from elements $e=1,\ldots,m_a$ surrounding the node a:

$$V_a=\sum_{e=1}^{m_a} V_a^{(e)}, \quad V_a^{(e)}=\frac{V^{(e)}}{4} \tag{1}$$

The Jacobian over an element e is the ratio between the current and initial element volumes, and also represents the volumetric part of the deformation gradient $\mathbf{F}$ as:

$$J^{(e)}=\frac{v^{(e)}}{V^{(e)}}=\det(\mathbf{F}) \tag{2}$$

The isochoric component of the deformation gradient is therefore given by:

$$\hat{\mathbf{F}}=J^{-1/3}\mathbf{F} \tag{3}$$

DOI: 10.1002/cnm

The existence of a total elastic energy function is assumed, given as:

$$\Pi(\mathbf{x}) = \int_V \Psi(\mathbf{F})\,\mathrm{d}V = \int_V \hat{\Psi}(\hat{\mathbf{F}})\,\mathrm{d}V + \int_V U(J)\,\mathrm{d}V \tag{4}$$

where Ψ is the strain energy density function with an isochoric component $\hat{\Psi}$ and a volumetric component U. The volumetric component U can only be a function of the volumetric ratio J, with the simplest and most commonly used form incorporating the bulk modulus κ of the material:

$$U(J) = \frac{\kappa}{2}(J-1)^2 \tag{5}$$

The element pressure is defined as:

$$p^{(e)} = \left.\frac{\mathrm{d}U}{\mathrm{d}J}\right|_{J=J^{(e)}} = \kappa(J^{(e)}-1) \tag{6}$$

The volumetric virtual work for the standard linear tetrahedron is expressed as:

$$\delta W_{\mathrm{vol}} = \sum_{e=1}^{m} p^{(e)} v^{(e)} \mathrm{div}\,\delta\mathbf{v}^{(e)} \tag{7}$$

where $\delta\mathbf{v}$ are the virtual velocities and m is the number of elements in the mesh.

The volumetric components of the element internal nodal forces can be derived from the volumetric virtual work as:

$$\mathbf{T}_{\mathrm{vol}}^{(e)} = p^{(e)} v^{(e)} \nabla \mathbf{N}_a^{(e)} \tag{8}$$

with $\mathbf{N}_a$ the shape functions of the element.

The ANP formulation is obtained by assuming that the volume ratio J remains constant over the volume attached to each node, therefore, reducing the number of incompressibility constraints. The average nodal volumetric ratio is defined in terms of the current and initial nodal volumes, given by (1), as:

$$J_a = \frac{v_a}{V_a} \tag{9}$$

and the volumetric strain energy is approximated by summing the contribution of all the n nodes in the mesh:

$$\Pi_{\mathrm{vol}}(\mathbf{x}) = \sum_{a=1}^{n} U(J_a) V_a \tag{10}$$

If only one material is considered, the ANP can be defined as:

$$p_a = \left.\frac{\mathrm{d}U}{\mathrm{d}J}\right|_{J=J_a} = \kappa(J_a-1) \tag{11}$$

By differentiating the volumetric strain energy given by (10) in the direction of the virtual velocities, the volumetric internal virtual work is obtained as:

$$\delta W_{\mathrm{vol}} = \sum_{a=1}^{n} \sum_{e=1}^{m_a} \frac{1}{4} p_a v^{(e)} \mathrm{div}\,\delta\mathbf{v}^{(e)} = \sum_{e=1}^{m} \overline{p}^{(e)} v^{(e)} \mathrm{div}\,\delta\mathbf{v}^{(e)} \tag{12}$$

DOI: 10.1002/cnm

Therefore, the average element pressure can be defined as:

$$\overline{p}^{(e)} = \frac{1}{4} \sum_{a=1}^{4} p_a^{(e)} \tag{13}$$

The difference between the ANP element and the standard linear tetrahedral element is the usage of the average element pressure (13) instead of the element pressure (6) in the expression of the volumetric internal virtual work (and therefore in the computation of the volumetric components of the internal nodal forces).

In case of multiple material interfaces, the nodal pressure cannot be computed using (11), as it is not clear what bulk modulus κ should be used. For each material type i converging at node a, a different nodal volume is defined as:

$$v_a^{(i)} = \sum_{e=1}^{m_a^{(i)}} \frac{1}{4} v^{(e)} \tag{14}$$

where $m_a^{(i)}$ represents the number of elements of material type i sharing node a. A different nodal pressure is then evaluated for each material as

$$p_a^{(i)} = \kappa^{(i)} (J_a^{(i)} - 1) \tag{15}$$

When the pressures are averaged over an element, only those corresponding to the same element material are used.

2.2. IANP formulation

The different treatment of elements having different material types at the interface nodes leads to:

- implementation problems, as not all elements in the mesh are treated in the same manner;
- a weaker enforcement of the incompressibility constraints for the nodes belonging to material interfaces (the elements of different material type are treated separately).

We now demonstrate how both these problems can be eliminated. We start with the definition of the volumetric strain energy for one of the nodes a belonging to an interface between multiple materials:

$$\Pi_{\text{vol}}^{a}(\mathbf{x}) = \sum_{i=1}^{k_a} U(J_a^{(i)}) V_a^{(i)} \tag{16}$$

where k_a represents the number of different material types converging to node a.

Instead of considering different nodal pressure for the different material types, as given by (15), we will make the assumption that the nodal pressure is constant over the nodal volume. This assumption derives from the relation that exists between pressure and stress ($p = -\sigma_{ii}/3$) [16] and from the fact that at the interface between two different materials the stress in the materials should be the same.

Therefore, the nodal pressure for such a node is expressed as:

$$p_a = \kappa^{(1)} (J_a^{(1)} - 1) = \cdots = \kappa^{(k_a)} (J_a^{(k_a)} - 1) \tag{17}$$

DOI: 10.1002/cnm

This can be transformed to:

$$p_a = \kappa^{(1)} \frac{v_a^{(1)} - V_a^{(1)}}{V_a^{(1)}} = \cdots = \kappa^{(k_a)} \frac{v_a^{(k_a)} - V_a^{(k_a)}}{V_a^{(k_a)}}$$

$$= \frac{\sum_{i=1}^{k_a} \kappa^{(i)} (v_a^{(i)} - V_a^{(i)})}{\sum_{i=1}^{k_a} V_a^{(i)}} = \frac{\sum_{i=1}^{k_a} \kappa^{(i)} \frac{1}{4} \sum_{e=1}^{m_a^i} (v^{(e)} - V^{(e)})}{\sum_{i=1}^{k_a} \frac{1}{4} \sum_{e=1}^{m_a^i} V^{(e)}}$$

$$= \frac{\sum_{i=1}^{k_a} \sum_{e=1}^{m_a^i} \kappa^{(i)} (v^{(e)} - V^{(e)})}{\sum_{e=1}^{m_a} V^{(e)}} = \frac{\sum_{e=1}^{m_a} p^{(e)} V^{(e)}}{\sum_{e=1}^{m_a} V^{(e)}} = \frac{\sum_{e=1}^{m_a} p^{(e)} V^{(e)}}{4 V_a} \tag{18}$$

The volumetric internal virtual work for node a is given by:

$$\delta W_{\text{vol}}^a = D\Pi_{\text{vol}}^a[\delta \mathbf{v}] = \sum_{i=1}^{k_a} \left. \frac{\mathrm{d}U}{\mathrm{d}J} \right|_{J=J_a^{(i)}} V_a^{(i)} DJ_a^{(i)}[\delta \mathbf{v}]$$

$$= \sum_{i=1}^{k_a} p_a V_a^{(i)} DJ_a^{(i)}[\delta \mathbf{v}] = \sum_{i=1}^{k_a} p_a V_a^{(i)} \frac{1}{V_a^{(i)}} Dv_a^{(i)}[\delta \mathbf{v}]$$

$$= \sum_{i=1}^{k_a} p_a Dv_a^{(i)}[\delta \mathbf{v}] \tag{19}$$

By replacing (14) in (19), and considering, from [12], that

$$DJ^{(e)}[\delta \mathbf{v}] = J^{(e)} \operatorname{div} \delta \mathbf{v}^{(e)} \tag{20}$$

we obtain:

$$\delta W_{\text{vol}}^a = \sum_{i=1}^{k_a} p_a \frac{1}{4} \sum_{e=1}^{m_a^{(i)}} Dv^{(e)}[\delta \mathbf{v}] = \sum_{e=1}^{m_a} p_a \frac{1}{4} Dv^{(e)}[\delta \mathbf{v}]$$

$$= \sum_{e=1}^{m_a} p_a \frac{1}{4} V^{(e)} DJ^{(e)}[\delta \mathbf{v}] = \sum_{e=1}^{m_a} \frac{1}{4} p_a v^{(e)} \operatorname{div} \delta \mathbf{v}^{(e)} \tag{21}$$

Comparing (21) with (12), we observe that the volumetric internal virtual work for node a is computed in the same manner, and therefore the element pressure will be defined by relation (13). The only difference between the standard ANP element and the IANP element consists in the computation of nodal pressure.

In case of a node surrounded by elements made of the same material, the nodal pressure given by (18) can be reduced to:

$$p_a = \frac{\sum_{e=1}^{m_a} p^{(e)} V^{(e)}}{\sum_{e=1}^{m_a} V^{(e)}} = \frac{\sum_{e=1}^{m_a} \frac{1}{4} \kappa (v^{(e)} - V^{(e)})}{\sum_{e=1}^{m_a} \frac{1}{4} V^{(e)}}$$

$$= \kappa \frac{v_a - V_a}{V_a} = \kappa (J_a - 1) \tag{22}$$

and the pressure for the standard ANP element is obtained. Therefore, the standard and the IANP elements behave differently only for elements situated at an interface between different materials.

DOI: 10.1002/cnm

3. IMPLEMENTATION CONSIDERATIONS

3.1. The modified deformation gradient

The only difference between the (standard or improved) ANP element and the linear tetrahedral element consists in the way the pressure is computed. The internal forces derived from the isochoric component of the strain energy are the same for all these elements. These forces depend only on the isochoric part of the deformation gradient.

The volumetric components of the internal forces depend on the element pressure, as given by (8), whereas the element pressure depends only on the volumetric part of the deformation gradient (6).

We consider an existing implementation for a linear tetrahedral element, with the internal forces computed based on the volumetric and isochoric components of the deformation gradient. In order to obtain the internal forces corresponding to the ANP elements, the volumetric part of the deformation gradient can be modified in such a way that the desired pressure (corresponding to the ANP elements) is obtained. This pressure, given by (13), can therefore be replaced in (6) to obtain the modified volumetric part for the deformation gradient:

$$\overline{J}^{(e)} = \frac{\overline{p}^{(e)}}{\kappa} + 1 \tag{23}$$

The modified deformation gradient:

$$\overline{\mathbf{X}}^{(e)} = (\overline{J}^{(e)})^{1/3}\hat{\mathbf{X}} = (\overline{J}^{(e)})^{1/3}(J^{(e)})^{-1/3}\mathbf{X} \tag{24}$$

has the same isochoric part as the deformation gradient of the element, but the volumetric part is modified in such a way that the pressure computed from it will correspond to the ANP element.

The computation of the internal nodal forces (or stiffness matrix) can now be done in the usual manner, but using the modified deformation gradient instead of the normal deformation gradient for defining the strains. In this way, the existing material law implementation can be used, as demonstrated in the next section.

It is worth noting that if the standard ANP element is used, the modified volumetric part for the deformation gradient becomes, after replacing in (23) the average element pressure from (13) and the average nodal pressure from (11):

$$\overline{J}^{(e)} = \frac{1}{4}\sum_{a=1}^{4} J_a \tag{25}$$

Therefore, the computation of pressure is no longer needed for such an implementation.

3.2. Integration in the Total Lagrangian Explicit Dynamic (TLED) algorithm

The TLED algorithm is a very efficient explicit algorithm based on the Total Lagrangian formulation that can be used for surgical simulation. The basic algorithm is presented in [17]. The modified algorithm that can use the IANP element presented in this paper is presented below. The additional steps required are marked with a (+).

DOI: 10.1002/cnm

`Pre-computation stage`:

1. Load mesh and boundary conditions.
2. For each element, compute the determinant of the Jacobian $\det(\mathbf{J})$ and the spatial derivatives of shape functions $\partial\mathbf{h}$ (notation from [18] is used, where the left superscript represents the current time and the left subscript represents the time of the reference configuration -0, when Total Lagrangian formulation is used).
3. Compute the diagonal (constant) mass matrix ${}^0\mathbf{M}$.
4. (+) Compute the initial volumes associated with each node V_a using (1).

`Initialization`:

1. Initialize nodal displacement ${}^0\mathbf{u}=\mathbf{0}, {}^{-\Delta t}\mathbf{u}=\mathbf{0}$, apply load for the first time step: forces or/and prescribed displacements: ${}^{\Delta t}R_i^{(k)} \leftarrow R^{(k)}(\Delta t)$ or/and ${}^{\Delta t}u_i^{(k)} \leftarrow d(\Delta t)$.

`Time stepping`:

Loop over elements:

1. Take element nodal displacements from the previous time step.
2. Compute deformation gradient ${}^t_0\mathbf{X}$ and its determinant J.
3. (+) Compute current element pressure using (6).

(+) Compute nodal pressure using (18).

Loop over elements:

1. (+) Compute the ANP using (13).
2. (+) Compute the modified deformation gradient using (23) and (24).
3. Compute the 2nd Piola–Kirchoff stress (vector) ${}^t_0\overline{\mathbf{S}}$ using the given material law (based on the modified deformation gradient).
4. Compute the element nodal reaction forces using Gaussian quadrature.

Making a (time) step:

1. Obtain net nodal reaction forces at time t, ${}^t\mathbf{T}$.
2. Explicitly compute displacements using central difference formula

$$ {}^{t+\Delta t}u_i^{(k)} = \frac{\Delta t^2}{M_k}({}^tR_i - {}^tT_i^{(k)}) + 2{}^tu_i^{(k)} - {}^{t-\Delta t}u_i^{(k)} \tag{26} $$

   where M_k is a diagonal entry in kth row of the diagonalized mass matrix, R_i is an external nodal force, and Δt is the time step.
3. Apply load for next step: ${}^{t+\Delta t}R_i^{(k)} \leftarrow R^{(k)}(t+\Delta t)$ or/and ${}^{t+\Delta t}u_i^{(k)} \leftarrow d(t+\Delta t)$.

The needed modifications are easy to implement and do not require major changes in the existing algorithm. The performances of the modified algorithm are presented in the next section.

4. SIMULATION RESULTS

Because the only difference between the IANP element proposed in this paper and the standard ANP element consists in the way interfaces between different materials are handled, we designed

DOI: 10.1002/cnm

Table I. Material properties.

Property	Material 1	Material 2
Young's modulus E (Pa)	3000	30 000
Poisson ratio v	0.49	0.48
Density ρ (kg/m^3)	1000	1000

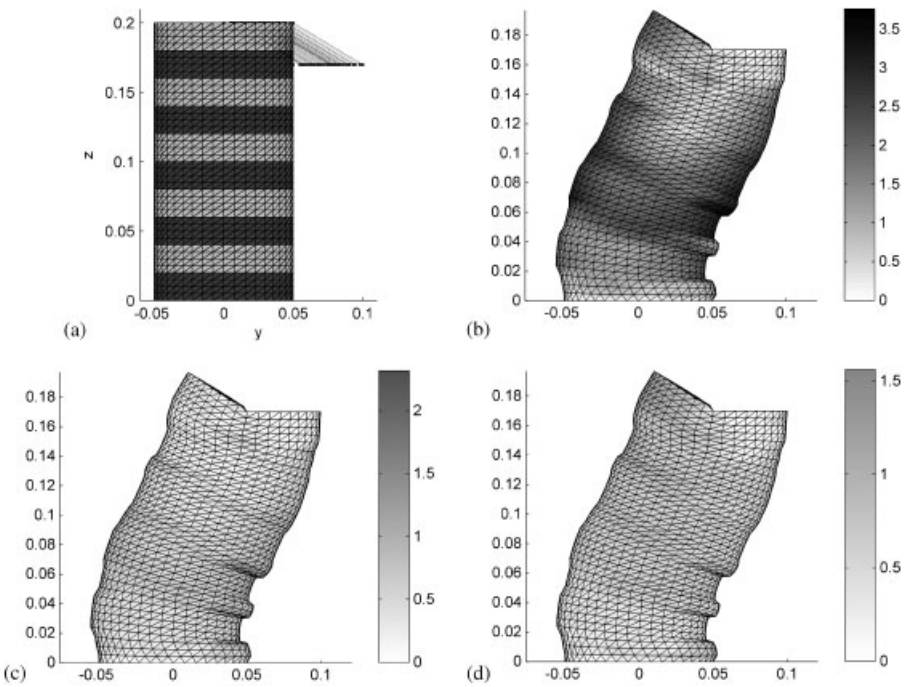

Figure 1. Deformation of a cylinder made out of section with different material properties: (a) the un-deformed configuration and the nodal displacements are applied. The color bars show the difference in positions of the surface nodes, in mm, between models using hexahedral elements and models using; (b) locking tetrahedral elements; (c) ANP elements; and (d) IANP elements.

a simulation experiment that highlights these differences. We considered a cylinder with a diameter of 0.1 m and a height of 0.2 m made out of alternating sections with two different material properties, as shown in Table I. We used a neo-Hookean material model for both materials.

Half of the nodes on the upper face of the cylinder were displaced in order to create a complex deformation field at the different material interfaces (Figure 1(a)).

Using the cylinder geometry, we created a hexahedral mesh (13 161 nodes and 12 000 elements) and a tetrahedral mesh (11 153 nodes and 60 030 elements). The behavior of the following elements was compared:

1. Fully integrated linear hexahedra, with selectively reduced integration of the volumetric term (Hexa), which should offer a benchmark solution [19];

DOI: 10.1002/cnm

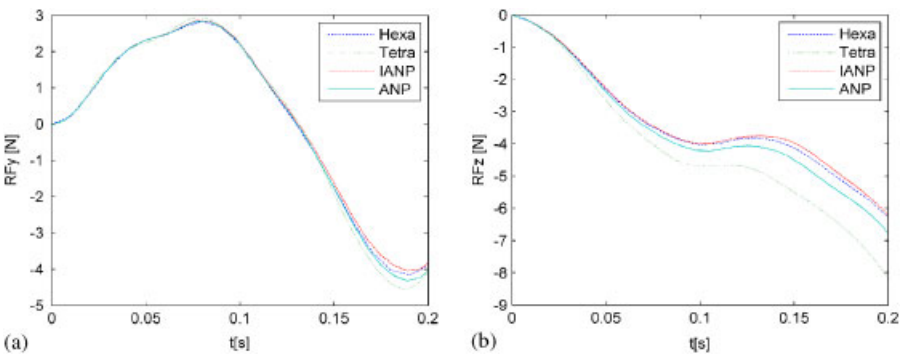

Figure 2. Reaction forces on the displaced face: (a) in the y direction and (b) in the z direction.

2. Standard ANP;
3. IANP, as developed in this paper;
4. Linear standard tetrahedron (Tetra).

All the computations were done using the TLED algorithm. Based on the displacement differences presented in Figure 1, we note the fact that the usage of standard locking tetrahedral elements can leads to errors of up to 3.8 mm in the deformation field. The use of ANP elements reduces the maximum error to 2.3 mm, whereas the use of IANP elements leads to a maximum error of 1.5 mm (all errors are considered relative to the results of the model that uses Hexa elements).

The reaction forces computed on the displaced face are presented in Figure 2. The results obtained using the IANP elements are the closest to the benchmark results given by the Hexa elements. Therefore, the IANP elements offer the best performances both in terms of displacements and reaction forces.

5. DISCUSSIONS AND CONCLUSIONS

An improvement of the ANP element is presented in this paper. This improved formulation handles all the elements of the mesh in the same manner (regardless of the fact they may be at an interface between materials), and therefore the use of different materials and the implementation in an existing finite element code can be made without difficulties.

The performance of the proposed IANP element is evaluated using the TLED algorithm against the standard tetrahedral element and the ANP element. The IANP element offered the best performances both in terms of displacements and reaction forces.

In an explicit code, the critical time step value for the ANP element is double compared with the critical time step for the standard locking tetrahedron in the one-dimensional case [20]. We observed a similar behavior for the ANP and IANP elements in the three-dimensional simulations. This means that we can use higher values for the time step in an explicit simulation using a mixed mesh, as the tetrahedral elements are usually the ones that impose the value of the critical time step. A higher critical time step leads to a reduction of the overall computation time.

DOI: 10.1002/cnm

ACKNOWLEDGEMENTS

The first author was an IPRS scholar in Australia during the completion of this research. The financial support of the Australian Research Council (Grant No. DP0343112, DP0664534 and LX0560460), NIH (Grant No. 1-RO3-CA126466-01A1), and UWA (Research Grant) is gratefully acknowledged.

REFERENCES

1. Owen SJ. A survey of unstructured mesh generation technology. *Proceedings of the 7th International Meshing Roundtable*, Dearborn, Michigan, U.S.A., 1998.
2. Viceconti M, Taddei F. Automatic generation of finite element meshes from computed tomography data. *Critical Reviews in Biomedical Engineering* 2003; **31**(1):27–72.
3. Owen SJ. Hex-dominant mesh generation using 3D constrained triangulation. *Computer-Aided Design* 2001; **33**:211–220.
4. Miller K. *Biomechanics of Brain for Computer Integrated Surgery*. Publishing House of Warsaw University of Technology: Warsaw, 2002.
5. Miller K, Chinzei K. Mechanical properties of brain tissue in tension. *Journal of Biomechanics* 2002; **35**:483–490.
6. Miller K *et al*. Mechanical properties of brain tissue in-vivo: experiment and computer simulation. *Journal of Biomechanics* 2000; **33**:1369–1376.
7. Miller K. Constitutive modelling of abdominal organs (Technical note). *Journal of Biomechanics* 2000; **33**: 367–373.
8. Miller K, Chinzei K. Constitutive modelling of brain tissue: experiment and theory. *Journal of Biomechanics* 1997; **30**(11/12):1115–1121.
9. Bilston LE, Liu Z, Phan-Tien N. Linear viscoelastic properties of bovine brain tissue in shear. *Biorheology* 1997; **34**(6):377–385.
10. Margulies SS, Thibault LE, Gennarelli TA. Physical model simulations of brain injury in the primate. *Journal of Biomechanics* 1990; **23**:823–836.
11. Bonet J, Burton AJ. A simple averaged nodal pressure tetrahedral element for incompressible and nearly incompressible dynamic explicit applications. *Communications in Numerical Methods in Engineering* 1998; **14**: 437–449.
12. Bonet J, Marriott H, Hassan O. An averaged nodal deformation gradient linear tetrahedral element for large strain explicit dynamic applications. *Communications in Numerical Methods in Engineering* 2001; **17**:551–561.
13. Zienkiewicz OC *et al*. Triangles and tetrahedra in explicit dynamic codes for solids. *International Journal for Numerical Methods in Engineering* 1998; **43**:565–583.
14. Dohrmann CR *et al*. Node-based uniform strain elements for three-node triangular and four-node tetrahedral meshes. *International Journal for Numerical Methods in Engineering* 2000; **47**:1549–1568.
15. Miller K *et al*. Total Lagrangian Explicit Dynamics Finite Element Algorithm for computing soft tissue deformation. *Communications in Numerical Methods in Engineering* 2007; **23**:121–134.
16. Hughes TJR. *The Finite Element Method*: *Linear Static and Dynamic Finite Element Analysis*. Dover Publications: Mineola, 2000.
17. Miller K, Joldes GR, Dane L. Total Lagrangian Explicit Dynamics Finite Element Algorithm for computing soft tissue deformation. *Communications in Numerical Methods in Engineering* 2007; **23**:121–134.
18. Bathe K-J. *Finite Element Procedures*. Prentice-Hall: New Jersey, 1996.
19. ABAQUS. *ABAQUS Theory Manual*, *Version 5.8*. Hibbitt, Karlsson & Sorensen, Inc.: Pawtucket, RI, 1998.
20. Bonet J, Marriott H, Hassan O. Stability and comparison of different linear tetrahedral formulations for nearly incompressible explicit dynamic applications. *International Journal for Numerical Methods in Engineering* 2001; **50**:119–133.

DOI: 10.1002/cnm